

SYSNO 1239355



**Instituto de Física  
Universidade de São Paulo**

**Neutrino oscillation parameters from MINOS,  
ICARUS and OPERA combined**

**Barger, V.<sup>1</sup>; Gago, A.M.<sup>2,3,4</sup>; Marfatia, D.<sup>1,5</sup>; Teves, W.J.C.<sup>3</sup>; Wood, B.P.<sup>1</sup> and  
Zukanovich Funchal, R.<sup>3</sup>**

<sup>1</sup> *Department of Physics, University of Wisconsin-Madison, WI 53706, USA*

<sup>2</sup> *Department of Physics, California State University, Dominguez Hills,  
Carson CA 90747, USA*

<sup>3</sup> *Instituto de Física, Universidade de São Paulo C.P. 66318, 05315-970,  
São Paulo, Brazil*

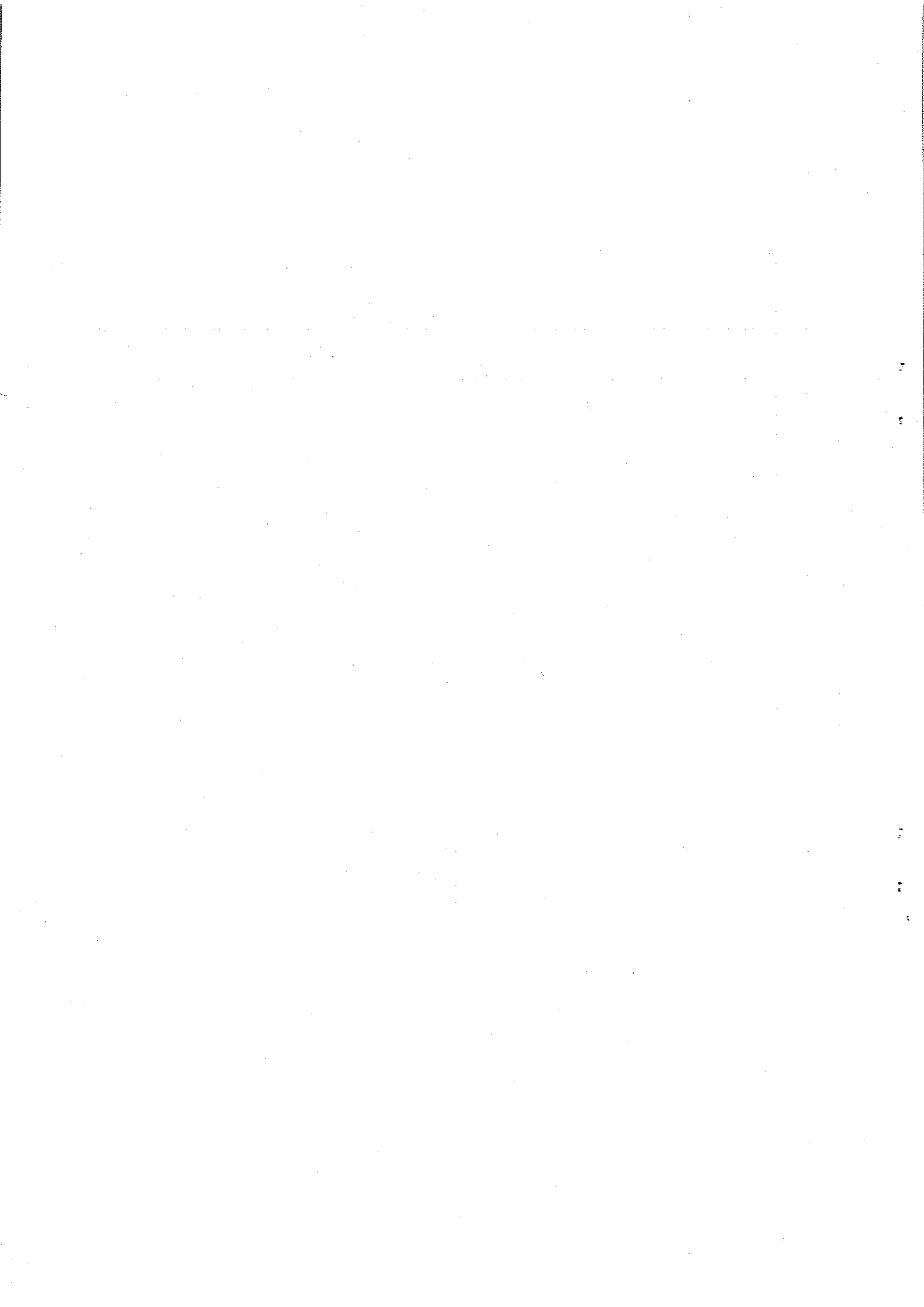
<sup>4</sup> *Sección Física, Departamento de Ciencias, Pontificia Universidad  
Católica del Perú, Apartado 1761, Lima, Perú*

<sup>5</sup> *Department of Physics, Boston University, Boston, MA 02215, USA*

**Publicação IF - 1528/2001**



UNIVERSIDADE DE SÃO PAULO  
Instituto de Física  
Cidade Universitária  
Caixa Postal 66.318  
05315-970 - São Paulo - Brasil



BU-01-26  
CSUDH-EPRG-01-05  
IFUSP-DFN/01-061  
MADPH-01-1242  
hep-ph/yymmnnn

## Neutrino oscillation parameters from MINOS, ICARUS and OPERA combined

V. Barger<sup>1</sup>, A. M. Gago<sup>2,3,4</sup>, D. Marfatia<sup>1,5</sup>, W. J. C. Teves<sup>3</sup>,  
B. P. Wood<sup>1</sup> and R. Zukanovich Funchal<sup>3</sup>

<sup>1</sup> Department of Physics, University of Wisconsin-Madison, WI 53706, USA

<sup>2</sup> Department of Physics, California State University, Dominguez Hills, Carson CA 90747, USA

<sup>3</sup> Instituto de Física, Universidade de São Paulo C. P. 66.318, 05315-970 São Paulo, Brazil

<sup>4</sup> Sección Física, Departamento de Ciencias, Pontificia Universidad Católica del Perú,  
Apartado 1761, Lima, Perú

<sup>5</sup> Department of Physics, Boston University, Boston, MA 02215, USA

### Abstract

We perform a detailed analysis of the capabilities of the MINOS, ICARUS and OPERA experiments to measure neutrino oscillation parameters at the atmospheric scale with their data taken separately and in combination. MINOS will determine  $\Delta m_{32}^2$  and  $\sin^2 2\theta_{23}$  to within 10% at the 99% C.L. with 10 kton-years of data. While no one experiment will determine  $\sin^2 2\theta_{13}$  with much precision, if its value lies in the combined sensitivity region of the three experiments, it will be possible to place a *lower bound* of  $\mathcal{O}(0.01)$  at the 95% C.L. on this parameter by combining the data from the three experiments. The same bound can be placed with a combination of MINOS and ICARUS data alone.

PACS numbers: 14.60.Pq, 12.15.Ff, 14.60.Lm

Typeset using REVTeX

## I. INTRODUCTION

The hypothesis that neutrino oscillations are responsible for the atmospheric [1–5] and solar [6–12] neutrino anomalies is becoming increasingly favored as more data is accumulated and new experiments start running. In particular, the disappearance of atmospheric  $\nu_\mu$  is currently being tested by K2K, the first long baseline experiment with confirming indications [13]. The best-fit oscillation parameters relevant to the atmospheric and solar scales from the analysis of the data from the above experiments are  $(\Delta m_{32}^2, \sin^2 2\theta_{23}) = (2.9 \times 10^{-3} \text{ eV}^2, 0.98)$  [14] and  $(\Delta m_{21}^2, \sin^2 2\theta_{12}) = (4.9 \times 10^{-5} \text{ eV}^2, 0.79)$  [15], respectively. Similar results were obtained in other global analyses of solar data; see Ref. [16]. The remaining mixing angle,  $\theta_{13}$ , is constrained by the CHOOZ experiment to be small,  $\sin^2 2\theta_{13} \lesssim 0.1$ , for values of  $\Delta m_{32}^2$  relevant to atmospheric neutrino oscillations at the 95% C.L. [17].

If oscillations in the three neutrino framework are assumed to be the correct solution to the solar and atmospheric neutrino problems (although the participation of a sterile neutrino in the oscillation dynamics, motivated by the LSND [18] data, is convincingly consistent with all existing data [19]), the mission of future experiments will be to precisely measure the relevant mixing parameters. The question of how well this task can be accomplished by the upcoming long baseline neutrino facilities is a rather important one since it will guide studies and set the goals for future neutrino experiments.

The KamLAND reactor experiment [20] will take important steps to solve the solar neutrino problem by determining if the large mixing angle MSW solution is correct, and by pinning down  $\Delta m_{21}^2$  and  $\sin^2 2\theta_{12}$  to accuracies of  $\mathcal{O}(10)\%$  if it is [21].

Low statistics in the K2K experiment will limit its power to measure the oscillation parameters relevant to the atmospheric neutrino problem. Three other long baseline accelerator neutrino experiments will address the atmospheric neutrino deficit with much higher statistics: the Main Injector Neutrino Oscillation Search (MINOS) experiment [22–24] from FNAL to the Soudan Mine, the Imaging Cosmic And Rare Underground Signals (ICARUS) experiment [25,26] and the Oscillation Project with Emulsion-tRacking Apparatus (OPERA) [27,28] from CERN to Gran Sasso. All are expected to start taking data around 2005, which will be long before the advent of superbeams [29] or neutrino factories [30]; for more references see Ref. [31]. These future long baseline experiments and KamLAND will therefore provide independent and accurate information about neutrino oscillation parameters at the solar and atmospheric scales with the important advantage that their results will not rely on assumptions about the solar model or the atmospheric neutrino fluxes.

In this work we explore the precision with which  $\Delta m_{32}^2$ ,  $\sin^2 2\theta_{23}$  and  $\sin^2 2\theta_{13}$  can be measured by MINOS, ICARUS and OPERA in the framework of three neutrino oscillations. We include all oscillation channels accessible to these experiments and take into account the available experimental information on backgrounds and efficiencies. All three experiments will operate with a high  $\nu_\mu$  flux and measure  $\nu_\mu$  disappearance. Because of the energy dependence of the oscillation probability, the most sensitive way of measuring the oscillation parameters is by studying the energy spectra of the neutrinos reaching the detector. Observations of an energy dependent distortion of the spectrum can uniquely determine the

oscillation parameters. Charged current events alone can provide information about the original  $\nu_\mu$  energy spectrum.

Although these experiments can also observe  $\nu_e$ , and to a lesser extent  $\nu_\tau$  appearance, the expected statistics in these channels are unlikely to be high enough to allow the energy spectra of these channels to be studied extensively. One can nevertheless extract important information from the total expected rates in these channels.

The paper is organized as follows. In Sec. II we very briefly review the three generation oscillation formalism. In Secs. III and IV we describe the MINOS, ICARUS, and OPERA experiments defining the observables relevant to our analyses and how they are calculated. In Sec. V we outline the procedure used to analyse the data simulated for MINOS, ICARUS and OPERA. We also perform a global analysis of the data from the three experiments. In Sec. VI we discuss our results on the sensitivity to and precision with which  $\Delta m_{32}^2$ ,  $\sin^2 2\theta_{23}$  and  $\sin^2 2\theta_{13}$  are expected to be determined by each experiment, and from the combined data of all three experiments. We present our conclusions in Sec. VII.

## II. 3 $\nu$ OSCILLATIONS

In the three generation framework there are three mixing angles and one  $CP$  phase that determine the amplitude for transition from flavor state to another. For the experiments under study, the  $CP$  phase has a negligible effect on the oscillation amplitudes and we set it to zero in what follows. The transformation between the neutrino mass eigenstates  $\nu_1$ ,  $\nu_2$  and  $\nu_3$  and neutrino interaction eigenstates  $\nu_e$ ,  $\nu_\mu$  and  $\nu_\tau$  is given by

$$\begin{pmatrix} \nu_e \\ \nu_\mu \\ \nu_\tau \end{pmatrix} = U \begin{pmatrix} \nu_1 \\ \nu_2 \\ \nu_3 \end{pmatrix} = \begin{bmatrix} c_{12}c_{13} & s_{12}c_{13} & s_{13} \\ -s_{12}c_{23} - c_{12}s_{23}s_{13} & c_{12}c_{23} - s_{12}s_{23}s_{13} & s_{23}c_{13} \\ s_{12}s_{23} - c_{12}c_{23}s_{13} & -c_{12}s_{23} - s_{12}c_{23}s_{13} & c_{23}c_{13} \end{bmatrix} \begin{pmatrix} \nu_1 \\ \nu_2 \\ \nu_3 \end{pmatrix}, \quad (2.1)$$

using the standard parameterization for the mixing matrix  $U$  [32]. Here  $c_{ij}$  and  $s_{ij}$  denote the cosine and the sine of the mixing angle  $\theta_{ij}$ .

The propagation of neutrinos through matter [33] is described by the evolution equation

$$i \frac{d}{dr} \begin{pmatrix} \nu_e \\ \nu_\mu \\ \nu_\tau \end{pmatrix} = \frac{1}{2E_\nu} \left[ U \begin{pmatrix} \Delta m_{21}^2 & 0 & 0 \\ 0 & 0 & 0 \\ 0 & 0 & \Delta m_{32}^2 \end{pmatrix} U^\dagger + \begin{pmatrix} A_e(r) & 0 & 0 \\ 0 & 0 & 0 \\ 0 & 0 & 0 \end{pmatrix} \right] \begin{pmatrix} \nu_e \\ \nu_\mu \\ \nu_\tau \end{pmatrix}, \quad (2.2)$$

where  $\Delta m_{ij}^2 = m_i^2 - m_j^2$  and  $E_\nu$  is the neutrino energy. Here,  $A_e(r) = 2\sqrt{2} G_F n_e(r) E_\nu = 1.52 \times 10^{-4} \text{ eV}^2 Y_e \rho (\text{g/cm}^3) E_\nu (\text{GeV})$  is the amplitude for  $\nu_e - e$  forward scattering in matter with  $Y_e$  denoting the electron fraction and  $\rho$  the matter density. For the experiments considered in this work, the neutrino path only traverses the Earth's crust which has an almost constant density of  $\rho \sim 3 \text{ g/cm}^3$  with  $Y_e \sim 0.5$ , giving  $A_e \sim 0.23 \times 10^{-3} \text{ eV}^2 E_\nu (\text{GeV})$ . Although analytical expressions for the oscillation probabilities in matter of constant density exist [34], we will solve Eq. (2.2) numerically taking into account the dependence of density on depth using the density profile from the Preliminary Reference Earth Model [35].

Since the baseline of the experiments under consideration is 730 km, and  $|\Delta m_{21}^2| \ll |\Delta m_{32}^2|$ , the contribution to the neutrino dynamics from the solar scale is small and the oscillation probabilities can be described in terms of just three parameters:  $\Delta m_{32}^2$ ,  $\sin^2 2\theta_{23}$ , and  $\sin^2 2\theta_{13}$ . For a constant matter density one can approximate the probability that a muon neutrino is converted to an electron neutrino as [34]

$$P_{\nu_\mu \rightarrow \nu_e} \approx \sin^2 2\theta_{13}^m \sin^2 \theta_{23} \sin^2 \left( \frac{\Delta m_{32}^2 L}{4E} S \right), \quad (2.3)$$

where

$$S = \sqrt{\left( \frac{A_e}{\Delta m_{32}^2} - \cos 2\theta_{13} \right)^2 + \sin^2 2\theta_{13}}, \quad (2.4)$$

and

$$\sin^2 2\theta_{13}^m = \frac{\sin^2 2\theta_{13}}{\left( \frac{A_e}{\Delta m_{32}^2} - \cos 2\theta_{13} \right)^2 + \sin^2 2\theta_{13}}. \quad (2.5)$$

For  $L \sim 730$  km, matter effects make a negligible contribution to the probability for conversion into a tau neutrino and the vacuum expression serves as a good approximation,

$$P_{\nu_\mu \rightarrow \nu_\tau} \approx \sin^2 2\theta_{23} \cos^4 \theta_{13} \sin^2 \left( \frac{\Delta m_{32}^2 L}{4E} \right). \quad (2.6)$$

From Eq. (2.3) one can see that the conversion probability for  $\nu_\mu \rightarrow \nu_e$  is approximately proportional to  $\sin^2 2\theta_{13}$  and is therefore small unless there is a resonant enhancement at  $\cos 2\theta_{13} = A_e/\Delta m_{32}^2$ . The  $\nu_\mu \rightarrow \nu_\tau$  conversion probability is, on the other hand, proportional to  $\sin^2 2\theta_{23}$ , and is therefore large. The survival probability,  $P_{\nu_\mu \rightarrow \nu_\mu} = 1 - P_{\nu_\mu \rightarrow \nu_\tau} - P_{\nu_\mu \rightarrow \nu_e}$  depends almost entirely on  $\sin^2 2\theta_{23}$  and  $\Delta m_{32}^2$ . Thus the parameters  $\sin^2 2\theta_{23}$  and  $\Delta m_{32}^2$  can be studied via  $\nu_\mu$  disappearance or  $\nu_\tau$  appearance, while  $\nu_e$  appearance is necessary to probe  $\sin^2 2\theta_{13}$ . The parameters  $\sin^2 2\theta_{23}$  and  $\Delta m_{32}^2$  should be readily accessible in all three experiments given the high event rates in the  $\nu_\mu \rightarrow \nu_\mu$  channel with  $\nu_\tau$  detection also possible in both ICARUS and OPERA. Because of the expected smallness of  $\sin^2 2\theta_{13}$  and the  $\nu_e$  background in the beam,  $\nu_e$  appearance will be difficult to study, and the accessibility to  $\sin^2 2\theta_{13}$  depends strongly on the detector.

### III. MINOS EXPERIMENT

The MINOS experiment [22] is designed to detect neutrinos from the Fermilab NuMI beam. The source of the neutrino beam is the decay of pions and kaons produced by collisions of 120 GeV protons (originating from the Fermilab Main Injector) with a nuclear target. A total of  $3.7 \times 10^{20}$  protons on target are expected per year. The beam will be almost exclusively  $\nu_\mu$  with a  $(\nu_e + \bar{\nu}_e)$  contamination of about 1%. A low, medium, or high



energy neutrino beam can be realized at MINOS by adjusting a focusing horn at the source. The resulting beam energies are peaked at approximately 3, 7 and 15 GeV, respectively. For MINOS to operate as a  $\nu_\tau$  appearance experiment either the high or medium energy beam would be required, since the  $\tau$  production threshold is 3.1 GeV. The experiment will most likely start with the low energy configuration, since this configuration will maximize its sensitivity to lower values of  $\Delta m_{32}^2$ , that are favored by the latest Super-Kamiokande and K2K results [14]. We do not include the effects of a hadronic hose or beamplug as these options are unlikely to be realized.

There will be two iron/scintillator detectors associated with the MINOS beam. The 1 kton near detector, which will detect neutrinos before oscillations occur, will be located on site at Fermilab. The 5.4 kton far detector will be located 732 km away from the source in the Soudan mine in Minnesota. It is expected that the experiment will run for two to three years starting in 2005.

MINOS will independently measure the rates and the energy spectra for muonless ( $0\mu$ ) and single-muon ( $1\mu$ ) events, which are related to the neutral current (nc) and charged current (cc) reactions, respectively [36]. The  $0\mu$  and  $1\mu$  event rates can be used to measure the ratio of neutral current events to charged current events which is an important consistency check on neutrino oscillations and could be useful for determining if a sterile neutrino is involved in the disappearance channel. However, it does not enhance the precision with which the oscillation parameters can be extracted. Since our goal is to determine the precision with which the oscillation parameters can be found in a three neutrino framework, it is a sound assumption that  $\nu_\mu$  disappearance is a consequence of transitions to  $\nu_\tau$ . We do not consider  $0\mu$  events in what follows.

We assume the low energy beam configuration to study the MINOS sensitivity to  $\Delta m_{32}^2$ ,  $\sin^2 2\theta_{23}$  and  $\sin^2 2\theta_{13}$ . We focus on  $\nu_\mu \rightarrow \nu_\mu$  disappearance to calculate the  $1\mu$ -event energy spectrum of charged current  $\nu_\mu$  events and  $\nu_\mu \rightarrow \nu_e$  appearance to calculate the total integrated rate of charged current  $\nu_e$  interactions.

The  $1\mu$ -event energy spectrum is divided into 23 bins of variable width  $\Delta E_i$ , according to the method described in Ref. [37]. The  $1\mu$ -event sample at MINOS will consist mainly of cc-events, with a small contribution coming from the misidentification of nc-events as cc-events. Thus, the content of the  $i^{\text{th}}$  bin,  $dN_{1\mu}^i/dE$ , is given by

$$\frac{dN_{1\mu}^i}{dE}(\Delta m_{32}^2, \sin^2 2\theta_{23}, \sin^2 2\theta_{13}) = \frac{A}{\Delta E_i} \int_{E_i - \frac{\Delta E_i}{2}}^{E_i + \frac{\Delta E_i}{2}} \phi_{\nu_\mu}(E) \left[ \sigma_{\nu_\mu}^{\text{cc}}(E) P_{\nu_\mu \rightarrow \nu_\mu}(E) \epsilon^{\text{cc}}(E) + \sigma_{\nu}^{\text{nc}}(E) \eta^{\text{nc}}(E) \right] dE. \quad (3.1)$$

Here,  $\phi_{\nu_\mu}$  is the neutrino flux at the MINOS far detector. We use the energy spectrum for  $\nu_\mu$  cc-events in the MINOS far detector in Ref. [37]. The number of active targets is  $A = M 10^9 N_A n_p n_y$ , where  $M$  is the detector mass in kton,  $10^9 N_A$  is the number of nucleons per kton ( $N_A \equiv$  Avogadro's number),  $n_y$  is the number of years of data taking and  $n_p$  is the number of protons on target per year. The  $\nu_\mu$  charged current cross section,  $\sigma_{\nu_\mu}^{\text{cc}}$ , and the neutral current cross section,  $\sigma_{\nu}^{\text{nc}}$ , are provided in Ref. [38] and Ref. [39], respectively. Here,  $\epsilon^{\text{cc}}$  is the probability that a given charged current  $\nu_\mu$  event will be correctly labelled

( $\sim 80\%$  at the spectral peak), and  $\eta^{\text{nc}}$  is the probability of misidentifying a given neutral current event as a  $1\mu$  event ( $\sim 10\%$  at the spectral peak). These factors were estimated by the MINOS collaboration using a detailed Monte Carlo simulation of the detector with the low energy beam configuration [40]. The Standard Model expectation at the far detector is about 400 single-muon events per kton-year.

The MINOS experiment will reduce the systematic errors associated with the charged current energy spectrum by comparing the spectrum measured at the far detector with that measured at the near detector from the same beam. The uncertainties in the far/near ratio, mainly due to the theoretical uncertainties in the secondary production of  $\pi$  and  $K$  in the NuMI target, range from 1-4% in the peak of the low energy beam up to 5-10% in the high energy tail [37]. We have neglected these errors in our study.

The  $\nu_e$  rate is defined as

$$R_e(\Delta m_{32}^2, \sin^2 2\theta_{23}, \sin^2 2\theta_{13}) = S_e + B_e^{(\mu\tau)} + B_e^{(\mu\mu)} + B_e^{(\text{beam})} + B_e^{(\text{nc})}, \quad (3.2)$$

where the signal,  $S_e$ , is

$$S_e(\Delta m_{32}^2, \sin^2 2\theta_{23}, \sin^2 2\theta_{13}) = A \int \phi_{\nu_\mu}(E) P_{\nu_\mu \rightarrow \nu_e}(E) \sigma_{\nu_e}^{\text{cc}}(E) \epsilon_e dE. \quad (3.3)$$

Here,  $\epsilon_e = 0.28$  is the signal efficiency and  $\sigma_{\nu_e}^{\text{cc}}$  is the  $\nu_e$  charged current cross section [38]. The electron background event contribution from the decay of tau leptons in the detector is

$$B_e^{(\mu\tau)}(\Delta m_{32}^2, \sin^2 2\theta_{23}, \sin^2 2\theta_{13}) = A \int \phi_{\nu_\mu}(E) P_{\nu_\mu \rightarrow \nu_\tau}(E) \sigma_{\nu_\tau}^{\text{cc}}(E) \epsilon_R^{(\mu\tau)} dE, \quad (3.4)$$

where  $\epsilon_R^{(\mu\tau)} = 0.066$  is the reduction efficiency and  $\sigma_{\nu_\tau}^{\text{cc}}$  is the  $\nu_\tau$  charged current cross section [38]. The background from  $e/\mu$  misidentification is given by

$$B_e^{(\mu\mu)}(\Delta m_{32}^2, \sin^2 2\theta_{23}, \sin^2 2\theta_{13}) = A \int \phi_{\nu_\mu}(E) P_{\nu_\mu \rightarrow \nu_\mu}(E) \sigma_{\nu_\mu}^{\text{cc}}(E) \eta^{(\mu\mu)} dE, \quad (3.5)$$

where  $\eta^{(\mu\mu)} = 0.001$  is the misidentification probability. The background coming from the  $\nu_e$  beam contamination is

$$B_e^{(\text{beam})}(\Delta m_{32}^2, \sin^2 2\theta_{23}, \sin^2 2\theta_{13}) = A \int \phi_{\nu_e}(E) P_{\nu_e \rightarrow \nu_e}(E) \sigma_{\nu_e}^{\text{cc}}(E) \epsilon_R^{(\text{beam})} dE, \quad (3.6)$$

where  $\epsilon_R^{(\text{beam})} = 0.079$  is the reduction efficiency. The final background included,  $B_e^{(\text{nc})}$ , from the decay of neutral pions created by neutral current interactions, is

$$B_e^{(\text{nc})}(\Delta m_{32}^2, \sin^2 2\theta_{23}, \sin^2 2\theta_{13}) = A \int \phi_{\nu_\mu}(E) \sigma_\nu^{\text{nc}}(E) \epsilon_R^{(\text{nc})} dE, \quad (3.7)$$

where  $\epsilon_R^{(\text{nc})} = 0.016$  is the reduction efficiency. The efficiencies used in calculating both the signal and the backgrounds for MINOS  $\nu_e$  events can be found in Ref. [41].

#### IV. CERN-GRAN SASSO EXPERIMENTS

A new facility under construction at CERN will direct a  $\nu_\mu$  beam 732 km to the Gran Sasso Laboratory in Italy where it will be intercepted by two massive detectors, ICARUS and OPERA. The number of protons on target at the CERN SPS source is expected to be  $4.5 \times 10^{19}$  per year, and the  $\nu_\mu$  beam will have an average energy of 17 GeV. The fractions  $\nu_e/\nu_\mu$ ,  $\nu_\mu/\nu_\mu$  and  $\nu_\tau/\nu_\mu$  in the beam are expected to be as low as 0.8%, 2% and  $10^{-7}$ , respectively.

The ICARUS [25] detector will use liquid argon for its detection medium, and is expected to have an initial effective volume of 3 ktons with a 10 year running time. We conservatively assume an exposure of 20 kton-years because more data than this does not significantly improve either the reach of the experiment or the precision with which the oscillation parameters are determinable. OPERA [27], another detector at the Gran Sasso consists of lead plates interspaced with emulsion sheets, and is expected to have an effective volume of 2 kton and a running time of 5 years.

We investigate the capabilities of ICARUS and OPERA as  $\nu_\mu$  disappearance,  $\nu_e$  appearance, and  $\nu_\tau$  appearance experiments. We calculate the full energy spectrum for the charged current  $\nu_\mu$  events, and rates for the charged current  $\nu_e$  and  $\nu_\tau$  events. Low statistics in the  $\nu_e$  and  $\nu_\tau$  appearance channels makes a study of their full energy spectra unfeasible. The  $\nu_\mu$  scattering energy spectra in ICARUS and OPERA consists of 16 bins of width  $\Delta E = 2.5$  GeV. The number of events in the  $i^{\text{th}}$  bin,  $dN_\mu^i/dE$ , is calculated as

$$\frac{dN_\mu^i}{dE}(\Delta m_{32}^2, \sin^2 2\theta_{23}, \sin^2 2\theta_{13}) = \frac{A}{\Delta E} \int_{E_i-1.25 \text{ GeV}}^{E_i+1.25 \text{ GeV}} \phi_{\nu_\mu}(E) P_{\nu_\mu \rightarrow \nu_\mu}(E) \sigma_{\nu_\mu}^{\text{cc}}(E) \epsilon(E) dE, \quad (4.1)$$

where  $\phi_{\nu_\mu}$  is the flux of  $\nu_\mu$  arriving at the Gran Sasso laboratory and  $\sigma_{\nu_\mu}^{\text{cc}}$  is the charged current cross section for  $\nu_\mu$ -nucleon scattering, both of which are available in Ref. [42]. Again,  $A$  is the number of active targets in the detector, and we assume a constant efficiency  $\epsilon = 0.98$  (0.94) for ICARUS (OPERA) according to Refs. [25,43] and [28], respectively. If no oscillations occur, 2180 (2070)  $\nu_\mu$  charged current events per kton-year are expected at the ICARUS (OPERA) detectors.

The  $\nu_\tau$  production rate at ICARUS,  $R_\tau$ , is

$$R_\tau(\Delta m_{32}^2, \sin^2 2\theta_{23}, \sin^2 2\theta_{13}) = S_\tau + B_\tau^{(\mu e)} + B_\tau^{(\text{beam})}, \quad (4.2)$$

where the signal,  $S_\tau$ , is defined as

$$S_\tau(\Delta m_{32}^2, \sin^2 2\theta_{23}, \sin^2 2\theta_{13}) = A \int \phi_{\nu_\mu}(E) P_{\nu_\mu \rightarrow \nu_\tau}(E) \sigma_{\nu_\tau}^{\text{cc}}(E) \epsilon_\tau dE, \quad (4.3)$$

and we use an overall efficiency  $\epsilon_\tau = 0.06$  [25,43]. Here we have assumed that the  $\tau$  identification at ICARUS will be made via the  $\tau \rightarrow e$  leptonic decay only [26,43,44]. The overall efficiency therefore includes the branching ratio which is  $\sim 18\%$  and the selection cuts efficiency.

Since tau events will be detected via an electron final state at ICARUS,  $\nu_e$  backgrounds in the beam must be considered for this experiment. One source is  $\nu_\mu \rightarrow \nu_e$  oscillations, and is given by

$$B_{\tau}^{(\mu e)}(\Delta m_{32}^2, \sin^2 2\theta_{23}, \sin^2 2\theta_{13}) = A \int \phi_{\nu_{\mu}}(E) P_{\nu_{\mu} \rightarrow \nu_e}(E) \sigma_{\nu_e}^{cc}(E) \epsilon_{\text{R}}^{(\mu e)} dE. \quad (4.4)$$

Another important background contribution comes from the intrinsic  $\nu_e$  beam contamination, and is given by

$$B_{\tau}^{(\text{beam})}(\Delta m_{32}^2, \sin^2 2\theta_{23}, \sin^2 2\theta_{13}) = A \int \phi_{\nu_e}(E) P_{\nu_e \rightarrow \nu_e}(E) \sigma_{\nu_e}^{cc}(E) \epsilon_{\text{R}}^{(\text{beam})} dE. \quad (4.5)$$

The reduction efficiencies are  $\epsilon_{\text{R}}^{(\mu e)} = 0.15$  and  $\epsilon_{\text{R}}^{(\text{beam})} = 0.009$  [43,44].

For the OPERA experiment, we have assumed  $\tau$  detection via its one-prong decay into leptons ( $l$ ) and hadrons ( $h$ ) [28]. Backgrounds can be safely neglected, and the integrated rate of charged current  $\nu_{\tau}$  interactions at OPERA is given by Eq. (4.3) with  $\epsilon_{\tau} = 0.087$ . This efficiency value includes  $\sum_{i=l,h} \text{Br}(\tau \rightarrow i)$  as well as the selection cuts efficiency [28].

The expression for the  $\nu_e$  production rate at ICARUS and OPERA,  $R_e$ , is identical to the one presented in Eq. (3.2) with the appropriate fluxes, cross sections, and efficiencies. For ICARUS,  $\epsilon_e = 0.75$ ,  $\epsilon_{\text{R}}^{(\mu\tau)} = 0.14$ ,  $\eta^{(\mu\mu)} = 0.002$ ,  $\epsilon_{\text{R}}^{(\text{beam})} = 0.19$  and  $\epsilon_{\text{R}}^{(\text{nc})} = 0.01$  so as to emulate the effect of the selection cuts of Ref [26]. The corresponding parameters for OPERA are  $\epsilon_e = 0.7$ ,  $\epsilon_{\text{R}}^{(\mu\tau)} = 0.13$  (which reproduces the electron detection efficiency of Ref. [27]),  $\eta^{(\mu\mu)} = 0.002$ ,  $\epsilon_{\text{R}}^{(\text{beam})} = 0.19$  and  $\epsilon_{\text{R}}^{(\text{nc})} = 0.016$ .

## V. DATA SIMULATION AND ANALYSIS

In this section we describe the procedures used to determine the sensitivity and contour plots for the three experiments and their combination.

### A. $\chi^2$ DEFINITIONS

#### 1. $\nu_{\mu} \rightarrow \nu_{\mu}$

For this oscillation channel we use the information from the  $\nu_{\mu}$  charged current energy spectrum of each experiment. All three experiments will observe large numbers of events of this type, so that the number of events in each bin obeys Gaussian statistics. The  $\chi^2$  function is then defined as

$$\chi_{\mu}^2(\Delta m_{32}^2, \sin^2 2\theta_{23}, \sin^2 2\theta_{13}) = \sum_{i,j=1,n_{\beta}} (N_i^{\text{obs}} - N_i^{\text{th}}) \sigma_{ij}^{-2} (N_j^{\text{obs}} - N_j^{\text{th}}), \quad (5.1)$$

where  $N_i^{\text{th}}$  denotes the theoretical prediction for the number of events in bin  $i$  (for a given set of oscillation parameters), calculated according to Eq. (3.1) for MINOS and Eq. (4.1) for ICARUS and OPERA.  $N_i^{\text{obs}}$  denotes the "observed" number of events in bin  $i$ . The simulation of the data giving  $N_i^{\text{obs}}$  will be described in Section C. The number of bins is  $n_{\beta} = 23, 16$  and  $16$  for  $\beta = \text{MINOS, ICARUS}$  and  $\text{OPERA}$ , respectively. For MINOS, the error matrix is defined as  $\sigma_{ij}^2 = \delta_{ij} N_i^{\text{obs}} + (0.02)^2 N_i^{\text{obs}} N_j^{\text{obs}}$ , where the off-diagonal elements reflect a 2% overall flux uncertainty [45]. For ICARUS and OPERA we only consider statistical errors, yielding  $\sigma_{ij}^2 = \delta_{ij} N_i^{\text{obs}}$ .

### 2. $\nu_\mu \rightarrow \nu_e$

Gaussian statistics will also be realized in this channel. Even in the case of no oscillations the background contributes a sufficient number of events to  $R_e$  to warrant a Gaussian  $\chi^2$  function,

$$\chi_e^2(\Delta m_{32}^2, \sin^2 2\theta_{23}, \sin^2 2\theta_{13}) = \left( \frac{R_e^{\text{obs}} - R_e^{\text{th}}}{\sigma_e} \right)^2. \quad (5.2)$$

Here, the theoretical electron rate  $R_e^{\text{th}}$  is given by Eq. (3.2) with the appropriate experimental parameters (fluxes, efficiencies, etc) for the experiment under consideration. For MINOS, we define the error as  $\sigma_e^2 = R_e^{\text{obs}} + (\delta_{\text{sys}}^{\text{min}} \times R_e^{\text{obs}})^2$  assuming a global systematic error  $\delta_{\text{sys}}^{\text{min}} = 0.1$ . For ICARUS, we define the error as  $\sigma_e^2 = R_e^{\text{obs}} + (\delta_{\text{sys}}^{\text{ica}} \times B_e^{\text{(beam)}})^2$ , where only the  $\nu_e$  beam contamination has been considered as a source of significant uncertainty with  $\delta_{\text{sys}}^{\text{ica}} = 0.05$ . For OPERA, we use  $\sigma_e^2 = R_e^{\text{obs}} + (\delta_{\text{sys-I}}^{\text{ope}} \times B_e^{\text{(beam)}})^2 + (\delta_{\text{sys-II}}^{\text{ope}} \times B_e^{\text{(nc)}})^2$ , where  $B_e^{\text{(beam)}}$  and  $B_e^{\text{(nc)}}$  are the OPERA backgrounds produced by the  $\nu_e$  beam contamination and the misidentified neutral current interactions, respectively. Their associated systematic errors are given by  $\delta_{\text{sys-I}}^{\text{ope}} = 0.1$  and  $\delta_{\text{sys-II}}^{\text{ope}} = 0.2$ , as suggested in Ref. [27]. We neglect the errors arising from other components of the background.

### 3. $\nu_\mu \rightarrow \nu_\tau$

The number of detected events in this channel is likely to be small for both ICARUS and OPERA and so we use a  $\chi^2$  function consistent with a Poisson distribution,

$$\chi_\tau^2(\Delta m_{32}^2, \sin^2 2\theta_{23}, \sin^2 2\theta_{13}) = 2 \left[ (R_\tau^{\text{obs}} - R_\tau^{\text{th}}) + R_\tau^{\text{obs}} \ln \left( \frac{R_\tau^{\text{obs}}}{R_\tau^{\text{th}}} \right) \right]. \quad (5.3)$$

Here, the theoretical  $\nu_\tau$  rate  $R_\tau^{\text{th}}$  is calculated via Eq. (4.3), using the appropriate experimental parameters for ICARUS and OPERA. When the number of  $\nu_\tau$  event rates is greater than 5, we use a standard Gaussian  $\chi^2$  function given by

$$\chi_\tau^2(\Delta m_{32}^2, \sin^2 2\theta_{23}, \sin^2 2\theta_{13}) = \left( \frac{R_\tau^{\text{obs}} - R_\tau^{\text{th}}}{\sigma_\tau} \right)^2. \quad (5.4)$$

The errors considered in this case are purely statistical.

## B. REGIONS OF SENSITIVITY

For the  $\nu_\mu \rightarrow \nu_e$  channel, we calculate the sensitivity regions for MINOS, ICARUS and OPERA in the  $(\sin^2 2\theta_{13}, \Delta m_{32}^2)$  plane. The procedure used is to set  $R_e^{\text{obs}} =$

$R_e(\Delta m_{32}^2, \sin^2 2\theta_{23}, 0)$  with  $\sin^2 2\theta_{23} = 0.85^1$  or 1, and minimize the  $\chi^2$  function given in Eq. (5.2) with respect to the parameters  $\sin^2 2\theta_{13}$  and  $\Delta m_{32}^2$ . Curves are then drawn at  $\Delta\chi^2 = \chi^2 - \chi_{\min}^2 = 4.61$  corresponding to the 90% C.L.. The sensitivities are calculated for each experiment separately as well as for their combined potential by using the same procedure with  $\chi^2 = \chi_{e(\text{minos})}^2 + \chi_{e(\text{icarus})}^2 + \chi_{e(\text{opera})}^2$ .

We determine the sensitivity to  $\sin^2 2\theta_{23}$  and  $\Delta m_{32}^2$  in the  $\nu_\mu \rightarrow \nu_\mu$  channel for MINOS and in the  $\nu_\mu \rightarrow \nu_\tau$  channel for ICARUS and OPERA. For MINOS, we calculate  $N_i^{\text{obs}} = dN_{1\mu}^i/dE(\Delta m_{32}^2, 0, \sin^2 2\theta_{13})$  with  $\sin^2 2\theta_{13}$  set either to 0 or 0.1, its minimum or maximum allowed value. Equation (5.1) is then minimized with respect to  $\sin^2 2\theta_{23}$  and  $\Delta m_{32}^2$ , and the contour of constant  $\Delta\chi^2$  at the 90% C.L. is found. For ICARUS and OPERA, we set  $R_\tau^{\text{obs}} = R_\tau(\Delta m_{32}^2, 0, \sin^2 2\theta_{13})$  in Eq. (5.3)/(5.4), again with  $\sin^2 2\theta_{13} = 0$  or 0.1, minimize with respect to  $\sin^2 2\theta_{23}$  and  $\Delta m_{32}^2$  and trace contours of constant  $\Delta\chi^2$ . For the combined sensitivity of all three experiments, the same procedure is repeated with a global  $\chi^2$  defined as  $\chi^2 = \chi_{\mu(\text{minos})}^2 + \chi_{\tau(\text{icarus})}^2 + \chi_{\tau(\text{opera})}^2$ .

### C. PREDICTING THE ALLOWED REGIONS

To predict how accurately MINOS, ICARUS and OPERA will determine the neutrino oscillation parameters at the atmospheric scale, we simulate data sets for the three experiments assuming oscillations occur with

$$\begin{aligned} \Delta m_{32}^2 &= 3 \times 10^{-3} \text{ eV}^2, & \Delta m_{21}^2 &= 5 \times 10^{-5} \text{ eV}^2, \\ \sin^2 2\theta_{23} &= 1, & \sin^2 2\theta_{12} &= 0.8, & \sin^2 2\theta_{13} &= 0.05. \end{aligned} \quad (5.5)$$

All parameters other than  $\theta_{13}$  are close to the best-fit values from the current data. The value of  $\theta_{13}$  is chosen to lie within (or close to) the sensitivity regions of all three experiments under consideration while obeying the CHOOZ limit [17]. We have assumed a normal hierarchy ( $\Delta m_{32}^2 > 0$ ). Note that since matter effects are small at 730 km, the results for an inverted hierarchy will not be substantially different from that for a normal hierarchy.

Each simulated data point is generated by randomly choosing a point from a Gaussian or Poisson distribution associated with the number of events expected theoretically. This procedure is followed for the 23 bins of the MINOS  $\nu_\mu$  energy spectrum as well as the 16 bins of the ICARUS and OPERA  $\nu_\mu$  spectra, giving the  $N_i^{\text{obs}}$  of Eq. (5.1). This is also done for the  $\nu_e$  charged current rates of all three experiments, yielding the  $R_e^{\text{obs}}$  in Eq. (5.2), and the  $\nu_\tau$  charged current rates at ICARUS and OPERA, giving the  $R_\tau^{\text{obs}}$  of Eq. (5.3) or (5.4). In the case of the  $\nu_e$  and  $\nu_\tau$  rates where backgrounds are taken into consideration, the backgrounds and signals are calculated and simulated separately before being combined to give the rates used in the  $\chi^2$  analyses.

---

<sup>1</sup>This value is approximately the smallest value of  $\sin^2 2\theta_{23}$  allowed at the 99% C. L. by a combined analysis of SuperKamiokande and K2K data [14]. We conservatively assume that  $\theta_{23} < \pi/4$ . If the converse were true, the sensitivity to  $\sin^2 2\theta_{13}$  is greater than for  $\sin^2 2\theta_{23} = 1$ .

The allowed regions are calculated for the individual experiments by combining the information available from each channel and defining total  $\chi^2$  functions as follows:

$$\begin{aligned}\chi_{\text{minos}}^2(\Delta m_{32}^2, \sin^2 2\theta_{23}, \sin^2 2\theta_{13}) &= \chi_{\mu}^2 + \chi_e^2, \\ \chi_{\text{icarus}}^2(\Delta m_{32}^2, \sin^2 2\theta_{23}, \sin^2 2\theta_{13}) &= \chi_{\mu}^2 + \chi_e^2 + \chi_{\tau}^2, \\ \chi_{\text{opera}}^2(\Delta m_{32}^2, \sin^2 2\theta_{23}, \sin^2 2\theta_{13}) &= \chi_{\mu}^2 + \chi_e^2 + \chi_{\tau}^2.\end{aligned}\tag{5.6}$$

The  $\chi^2$  functions are then minimized by varying  $\Delta m_{32}^2$ ,  $\sin^2 2\theta_{23}$  and  $\sin^2 2\theta_{13}$  with  $\Delta m_{21}^2 = 5 \times 10^{-5} \text{ eV}^2$  and  $\sin^2 2\theta_{12} = 0.8$ . Contours of  $\Delta\chi^2 = 6.25$  and  $11.36$  are made corresponding to the 90% and 99% C.L., respectively. These confidence level regions are projected on to two-dimensional subspaces of the three parameter space.

To investigate whether combining data from the three experiments improves the determination of the oscillation parameters, we define a global  $\chi^2$  function as

$$\chi_{\text{minos+icarus+opera}}^2(\Delta m_{32}^2, \sin^2 2\theta_{23}, \sin^2 2\theta_{13}) = \chi_{\text{minos}}^2 + \chi_{\text{icarus}}^2 + \chi_{\text{opera}}^2.\tag{5.7}$$

This  $\chi^2$  function is minimized and contours are made as described above.

## VI. RESULTS

### A. MINOS

In Fig. 1 we present the sensitivity (at the 90% C.L.) of MINOS in the  $\nu_e$  appearance and  $\nu_{\mu}$  disappearance channels for an exposure of 10 kton-years. In the  $\nu_e$  appearance channel (left panel of Fig. 1), we see a small decrease in the sensitivity of MINOS as  $\sin^2 2\theta_{23}$  is decreased within its allowed range. MINOS is sensitive to  $\sin^2 2\theta_{13} \gtrsim 0.05$  for  $\Delta m_{32}^2 \sim 3 \times 10^{-3} \text{ eV}^2$  and maximal  $\nu_{\mu} - \nu_{\tau}$  mixing. For the  $\nu_{\mu}$  disappearance channel, one can see that the region of sensitivity is not affected by the variation of  $\sin^2 2\theta_{13}$  within its allowed range. MINOS is sensitive to  $\Delta m_{32}^2 \gtrsim 5 \times 10^{-4} \text{ eV}^2$  at maximal  $\sin^2 2\theta_{23}$ . The sensitivity of the neutral current to charged current event ratio to the leading oscillation parameters has been analyzed in Ref. [40]. That sensitivity is comparable to the sensitivity of the  $\nu_{\mu}$  disappearance channel in Fig. 1. We emphasize, however, that direct evidence for transitions to  $\nu_{\tau}$  is a very important aspect of the MINOS experiment, which can be accomplished by comparing the  $0\mu$  and  $1\mu$  event rates.

For the oscillation parameters of Eq. (5.5), the signal (background) is comprised of 2770 (0)  $\nu_{\mu}$  cc events and 15 (41)  $\nu_e$  events. Note that we have included the contribution from misidentified nc-events in the  $\nu_{\mu}$  event sample. In Fig. 2 we show the allowed regions obtained by simulating data for the MINOS detector. The  $\Delta\chi^2$  contours are shown at the 90 and 99% C.L.. Because of high statistics and an optimal L/E combination, MINOS should be able to pin down  $\Delta m_{32}^2$  and  $\sin^2 2\theta_{23}$  quite precisely, as is shown most clearly by the plot in the  $(\sin^2 2\theta_{23}, \Delta m_{32}^2)$  plane. For 10 kton-years of exposure, we find that MINOS should be able to measure these parameters to within 10% at the 99% C.L.. However, MINOS will not make a determination of  $\sin^2 2\theta_{13}$ . Low statistics in the  $\nu_e$  channel are expected because of the smallness of  $\theta_{13}$ , and relatively large backgrounds of  $\nu_e$  are expected to be present in the beam.

## B. ICARUS

The sensitivity of the ICARUS experiment to the  $\nu_\mu \rightarrow \nu_e$  and  $\nu_\mu \rightarrow \nu_\tau$  oscillation channels are shown in the left and right-hand panels of Fig. 3, respectively. 30 kton-years of exposure is assumed, and the contours are drawn at the 90 and 99% C.L.. For the  $\nu_e$  appearance channel, we find that ICARUS can access values of  $\sin^2 2\theta_{13} \gtrsim 0.03$  for  $\Delta m_{32}^2 \sim 3 \times 10^{-3} \text{ eV}^2$  and maximal  $\nu_\mu - \nu_\tau$  mixing. From the  $\nu_\tau$  appearance channel, we find that ICARUS is sensitive to  $\Delta m_{32}^2 \gtrsim 1 - 2 \times 10^{-3} \text{ eV}^2$  at maximal mixing.

The theoretical input (Eq. (5.5)) yields 41960 (0), 34 (380) and 27 (11)  $\nu_\mu, \nu_e, \nu_\tau$  signal (background) events, respectively. Figure 4 shows 90 and 99% C.L. contours obtained by simulating data for all three channels that can be studied by the ICARUS experiment by observing variations in  $\chi^2 = \chi_e^2 + \chi_\mu^2 + \chi_\tau^2$ . From the three panels displayed in the figure, it can be seen that ICARUS can determine  $\Delta m_{32}^2$  and  $\sin^2 2\theta_{23}$  to within 30% at the 99% C.L. but will not provide a meaningful determination of  $\sin^2 2\theta_{13}$ .

## C. OPERA

Figure 5 shows the sensitivity of the OPERA experiment to oscillation parameters at the atmospheric scale via the  $\nu_\mu \rightarrow \nu_e$  and  $\nu_\mu \rightarrow \nu_\tau$  channels, respectively. This plot is made for 10 kton-years of exposure, and represents the 90% C.L.. Using  $\nu_e$  appearance, we find that OPERA will be sensitive to values of  $\sin^2 2\theta_{13} \gtrsim 0.2$  for  $\Delta m_{32}^2 \sim 3 \times 10^{-3} \text{ eV}^2$  and maximal  $\nu_\mu - \nu_\tau$  mixing, but this region is ruled out by CHOOZ. Exploiting  $\nu_\tau$  appearance, OPERA is shown to be sensitive to  $\Delta m_{32}^2 \gtrsim 1 \times 10^{-3} \text{ eV}^2$  at maximal mixing independent of the value of  $\sin^2 2\theta_{13}$ . Although OPERA has no considerable background for  $\tau$  events as well as a higher detection efficiency than ICARUS, the latter has a greater sensitivity in this channel because of its larger volume and consequently higher event rate.

The number of  $\nu_\mu, \nu_e, \nu_\tau$  signal (background) events expected for the oscillation parameters used are 19870 (0), 14 (230) and 16 (0), respectively. In Fig. 6 we present contours of  $\Delta\chi^2$  at the 90 and 99% C.L. for OPERA.

## D. Global Analysis

In Fig. 7 we present the 90% C.L. sensitivity regions after combining the data simulated for the MINOS, ICARUS and OPERA experiments. In the  $(\sin^2 2\theta_{13}, \Delta m_{32}^2)$  plane, the combined sensitivity does not show much improvement over ICARUS alone, resulting in a sensitivity to  $\sin^2 2\theta_{13} \gtrsim 0.02$  for  $\Delta m_{32}^2 \sim 3 \times 10^{-3} \text{ eV}^2$  and maximal  $\nu_\mu - \nu_\tau$  mixing. The sensitivity of the experiments in the  $(\sin^2 2\theta_{23}, \Delta m_{32}^2)$  plane depends only slightly on the value of  $\sin^2 2\theta_{13}$  between 0 and 0.1. The combined sensitivity of the three experiments is  $\Delta m_{32}^2 \gtrsim 1 - 2 \times 10^{-3} \text{ eV}^2$  at maximal mixing which is worse than the sensitivity of MINOS. The low  $\nu_\tau$  event rates expected at ICARUS and OPERA corrupt the MINOS  $\nu_\mu$  disappearance signal at low values of  $\Delta m_{32}^2$ .



In Fig. 8 we show the allowed regions obtained from the combined analysis at the 90%, 95% and 99% C.L.. The precision with which the combination of the experiments can determine  $\Delta m_{32}^2$  and  $\sin^2 2\theta_{23}$  does not improve from the analysis with MINOS alone, since changes in  $\chi_{\text{minos}}^2$  dominates over any changes in the overall  $\chi^2$  function. These parameters can therefore be determined to within 10% once again. However, the ability of these experiments to constrain  $\sin^2 2\theta_{13}$  becomes feasible by combining them into a single analysis. For the data we simulated, we obtain  $\sin^2 2\theta_{13} \gtrsim 0.01$  at the 95% C.L.. Similar results for  $\sin^2 2\theta_{13}$  are obtained by setting  $\chi^2 = \chi_{\text{minos}}^2 + \chi_{\text{icarus}}^2$ , since only MINOS and ICARUS are sensitive to values of  $\sin^2 2\theta_{13} < 0.1$  for  $\Delta m_{32}^2 = 3 \times 10^{-3} \text{ eV}^2$ .

## VII. CONCLUSIONS

We have studied the potential of the future long baseline experiments ICARUS, MINOS, and OPERA, to ascertain the neutrino oscillation parameters at the atmospheric scale as separate experiments, and in combination. By simulating data at  $\Delta m_{32}^2 = 3 \times 10^{-3} \text{ eV}^2$ ,  $\Delta m_{12}^2 = 5 \times 10^{-5} \text{ eV}^2$ ,  $\sin^2 2\theta_{23} = 1$ ,  $\sin^2 2\theta_{12} = 0.8$  and  $\sin^2 2\theta_{13} = 0.05$  for all three experiments, and calculating the allowed regions given by this data, we have estimated the precision with which these experiments can determine the parameters  $\Delta m_{32}^2$ ,  $\sin^2 2\theta_{23}$ , and  $\sin^2 2\theta_{13}$ . We took into consideration  $\nu_\mu$  disappearance and  $\nu_e$  appearance for all three experiments and  $\nu_\tau$  appearance for ICARUS and OPERA.

The range of values of  $\Delta m_{32}^2$  and  $\sin^2 2\theta_{23}$  allowed by the Super-Kamiokande atmospheric neutrino data will be significantly narrowed by the MINOS experiment. With an optimal  $\langle L/E \rangle$  ratio for studying these parameters, MINOS should pin them down to within 10% at the 99% C.L. with 10 kton-years of data. ICARUS and OPERA, though not as sensitive to these parameters as MINOS, will provide an important check on the neutrino oscillation hypothesis by observing tau events via the  $\nu_\mu \rightarrow \nu_\tau$  channel. The value of  $\sin^2 2\theta_{13}$  will be difficult for these experiments to determine because of low event rates and large backgrounds in the  $\nu_e$  channel. We have shown that this parameter will remain unbounded when the experiments are analysed separately. Combining the data from the MINOS and ICARUS experiments may allow a lower bound on  $\sin^2 2\theta_{13}$  of  $\mathcal{O}(0.01)$  to be placed at the 95% C.L. if  $\sin^2 2\theta_{13}$  lies within the combined sensitivity of the experiments. Establishing a lower bound on  $\sin^2 2\theta_{13}$  would eliminate models that predict smaller values of  $\sin^2 2\theta_{13}$ . If  $\sin^2 2\theta_{13} > 0.01$  and the  $CP$  phase is sufficiently large,  $CP$  violation in the lepton sector could be studied at superbeam facilities [46].

In the next decade, with data from the three experiments considered (and a little luck), we could have good knowledge of the parameters that mediate atmospheric neutrino oscillations. Along with KamLAND's possible determination of  $\Delta m_{12}^2$  and  $\sin^2 2\theta_{12}$  using reactor neutrinos [21], all the elements of the mixing matrix other than the  $CP$  phase could be known.

## ACKNOWLEDGMENTS

We thank A. Bettini, A. Erwin, M. Goodman and D. Harris for discussions. We are grateful to M. Messier for providing us with the MINOS energy spectrum for the low energy beam and to D. A. Petyt for information on MINOS efficiencies. D. M. and B. P. W. thank Universidade de São Paulo for its hospitality during the initial stages of this work. This work was supported by Fundação de Amparo à Pesquisa do Estado de São Paulo (FAPESP), by Conselho Nacional de e Ciência e Tecnologia (CNPq), by a U.S. NSF grant INT-9805573, by Department of Energy grants DE-FG02-91ER40676 and DE-FG02-95ER40896 and by the University of Wisconsin Research Committee with funds granted by the Wisconsin Alumni Research Foundation.

## REFERENCES

- [1] Kamiokande Collaboration, H. S. Hirata *et al.*, Phys. Lett. B **205**, 416 (1988); *ibid.* **280**, 146 (1992); Y. Fukuda *et al.*, *ibid.* **335**, 237 (1994).
- [2] IMB Collaboration, R. Becker-Szendy *et al.*, Phys. Rev. D **46**, 3720 (1992).
- [3] MACRO Collaboration, M. Ambrosio *et al.*, Phys. Lett. B **478**, 5 (2000); B. C. Barish, Nucl. Phys. B (Proc. Suppl.) **91**, 141 (2001).
- [4] Soudan-2 Collaboration, W. W. M. Allison *et al.*, Phys. Lett. B **391**, 491 (1997); Phys. Lett. B **449**, 137 (1999); W. A. Mann, Nucl. Phys. B (Proc. Suppl.) **91**, 134 (2001).
- [5] The Super-Kamiokande Collaboration, Y. Fukuda *et al.*, Phys. Rev. Lett. **81**, 1562 (1998); H. Sobel, Nucl. Phys. B (Proc. Suppl.) **91**, 127 (2001).
- [6] Homestake Collaboration, K. Lande *et al.*, Astrophys. J. **496**, 505 (1998).
- [7] Kamiokande Collaboration, Y. Fukuda *et al.*, Phys. Rev. Lett. **77**, 1683 (1996).
- [8] GALLEX Collaboration, W. Hampel *et al.*, Phys. Lett. B **447**, 127 (1999).
- [9] GNO Collaboration, M. Altmann *et al.*, Phys. Lett. B **490**, 16 (2000).
- [10] SAGE Collaboration, J. N. Abdurashitov *et al.*, Phys. Rev. C **60**, 055801 (1999); V. N. Gavrin, Nucl. Phys. B (Proc. Suppl.) **91**, 36 (2001).
- [11] Y. Suzuki, Nucl. Phys. B (Proc. Suppl.) **91**, 29 (2001); Super-Kamiokande Collaboration, S. Fukuda *et al.*, hep-ex/0103032.
- [12] SNO Collaboration, Q. R. Ahmad *et al.*, Phys. Rev. Lett. **87**, 071301 (2001).
- [13] K2K Collaboration, S. H. Ahn, *et al.*, hep-ex/0103001.
- [14] G. L. Fogli, E. Lisi and A. Marrone, hep-ph/0110089.
- [15] G. L. Fogli, E. Lisi, D. Montanino and A. Palazzo, Phys. Rev. D **64**, 093007 (2001).
- [16] J. N. Bahcall, M. C. Gonzalez-Garcia and C. Pena-Garay, JHEP **0108**, 014 (2001); A. Bandyopadhyay, S. Choubey, S. Goswami and K. Kar, Phys. Lett. B **519**, 83 (2001).
- [17] M. Apollonio *et al.*, Phys. Lett. B **466**, 415 (1999).
- [18] LSND Collaboration, A. Aguilar *et al.*, hep-ex/0104049.
- [19] V. Barger, D. Marfatia and K. Whisnant, hep-ph/0106207; M. C. Gonzalez-Garcia, M. Maltoni and C. Pena-Garay, hep-ph/0108073.
- [20] A. Piepke for the KamLAND Collaboration, Nucl. Phys. B (Proc. Suppl.) **91**, 99 (2001).
- [21] V. Barger, D. Marfatia, and B. P. Wood, Phys. Lett. B **498**, 53 (2001).
- [22] The MINOS Collaboration, "Neutrino Oscillation Physics at Fermilab: The NuMI-MINOS Project", Fermilab Report No. NuMI-L-375 (1998).
- [23] S. G. Wojcicki for the MINOS Collaboration, Nucl. Phys. B (Proc. Suppl.) **91**, 216 (2001).
- [24] P. G. Harris, Fermilab Report No. NuMI-L-726 (2001).
- [25] The ICARUS Collaboration, *The ICARUS Experiment*, LNGS-P28/2001, LNGS-EXP 13/89 add.1/01, ICARUS-TM/2001, see <http://pcnometh4.cern.ch/publications.html>; see also the slides from IX International Workshop on "Neutrino Telescopes", Venice, Italy, March (2001).
- [26] A. Rubbia for the ICARUS Collaboration, talk given at Skandinavian Neutrino Workshop (SNOW), Uppsala, Sweden, February (2001), which are available at <http://pcnometh4.cern.ch/publicpdf.html>.

- [27] OPERA Collaboration, *The OPERA  $\nu_\tau$  appearance experiment in the CERN-Gran Sasso neutrino beam*, CERN/SPSC 98-25, SPSC/M612, LNGS-LOI 8/97, October, 1998.
- [28] OPERA Collaboration, *Experiment Proposal OPERA: An appearance experiment to search  $\nu_\mu \rightarrow \nu_\tau$  oscillations in the CNGS neutrino beam*, CERN/SPSC 2000-028, SPSC/P318, LNGS P25/2000, July, 2000.
- [29] V. Barger, S. Geer, R. Raja and K. Whisnant, Phys. Rev. D **63**, 113011 (2001); B. Richter, hep-ph/0008222; Y. Itow *et al.*, hep-ex/0106019.
- [30] S. Geer, Phys. Rev. D **57**, 6989 (1998); V. Barger, S. Geer and K. Whisnant, Phys. Rev. D **61**, 053004 (2000).
- [31] T. Adams *et al.*, *E1 Working Group Summary: Neutrino Factories and Muon Colliders in the Proceedings of Snowmass 2001*.
- [32] D. E. Groom *et al.* [Particle Data Group Collaboration], Eur. Phys. J. C **15**, 1 (2000).
- [33] V. Barger, K. Whisnant, S. Pakvasa and R. J. Phillips, Phys. Rev. D **22**, 2718 (1980).
- [34] J. Arafune, M. Koike and J. Sato, Phys. Rev. D **56**, 3093 (1997) [Erratum-ibid. D **60**, 119905 (1997)]; A. Cervera, A. Donini, M. B. Gavela, J. J. Gomez Cadenas, P. Hernandez, O. Mena and S. Rigolin, Nucl. Phys. B **579**, 17 (2000) [Erratum-ibid. B **593**, 731 (2000)]; M. Freund, Phys. Rev. D **64**, 053003 (2001).
- [35] A. Dziewonski and D. Anderson, Phys. Earth Planet. Inter. **25**, 297 (1981).
- [36] The MINOS Collaboration, P. Adamson *et al.*, Fermilab Report No. NuMI-L-337 (1998).
- [37] M. Messier *et al.*, Fermilab Report No. NuMI-B-700 (2001).
- [38] H. M. Gallagher, Ph.D. thesis, University of Minnesota, 1996, available at <http://hepunix.rl.ac.uk/soudan2/pubs/theses.html>.
- [39] M. D. Messier, Ph.D. thesis, Boston University, 1999, available at <http://hep.bu.edu/messier/>.
- [40] D. A. Petyt, Fermilab Report No. NuMI-L-481 (1999). We are using the new cc-efficiency and nc-contamination curves that were provided to us by D. A. Petyt.
- [41] M. Diwan, M. Messier, B. Viren, and L. Wai, Fermilab Report No. NuMI-L-714 (2001).
- [42] The charged current cross sections for  $\nu_\mu$  and  $\nu_\tau$  can be obtained in form of a table from <http://www.cern.ch/NGS>.
- [43] ICANOE Collaboration, *ICANOE, A proposal for a CERN-GS long baseline and atmospheric neutrino oscillation experiment*, INFN/AE-99-17, CERN/SPSC 99-25, SPSC/P314, August, 1999, see <http://pcnometh4.cern.ch/publications.html>.
- [44] A. Rubbia, Nucl. Phys. B (Proc. Suppl.) **91**, 223 (2001).
- [45] C. G. Arroyo, Fermilab Report No. NuMI-L-482 (1999).
- [46] V. Barger, D. Marfatia and K. Whisnant, hep-ph/0108090.

FIGURES

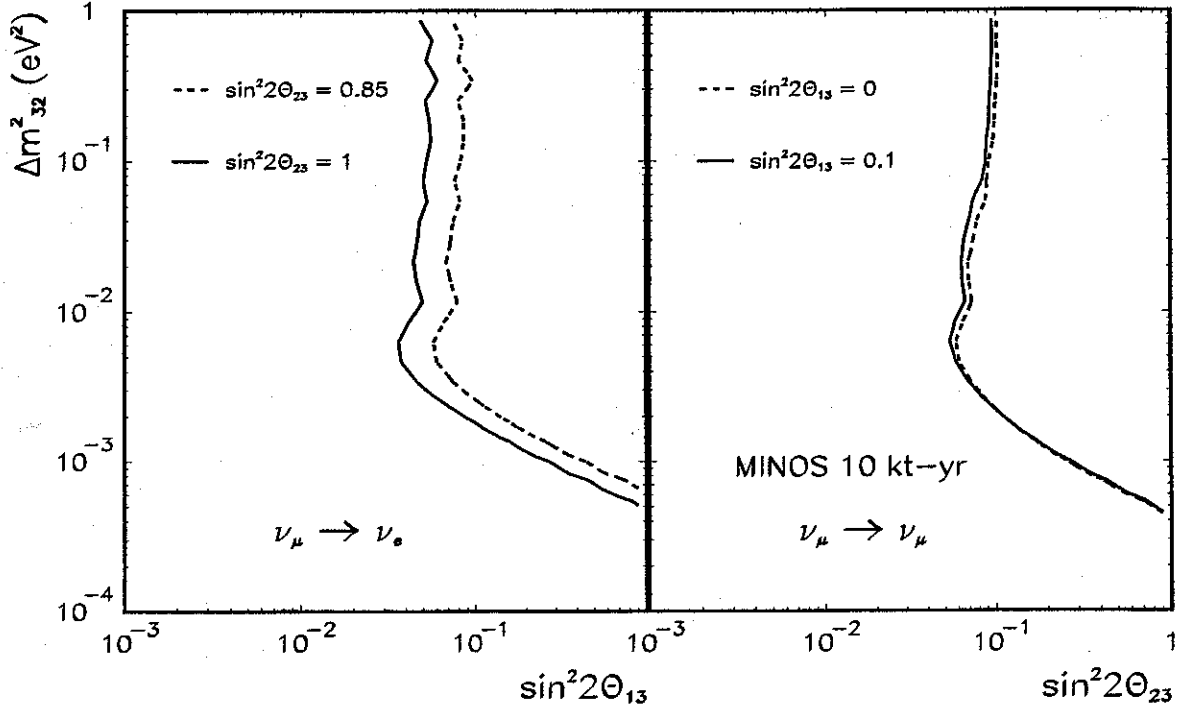


FIG. 1. MINOS sensitivities for the  $\nu_\mu \rightarrow \nu_e$  and  $\nu_\mu \rightarrow \nu_\mu$  channels at the 90% C.L.. The other oscillation parameters are fixed at  $\Delta m_{21}^2 = 5 \times 10^{-5}$  eV<sup>2</sup> and  $\sin^2 2\theta_{12} = 0.8$ , the best-fit solution to the solar neutrino problem. To determine the sensitivity to  $\sin^2 2\theta_{13}$  when  $\sin^2 2\theta_{23} = 0.85$ , we have taken  $\theta_{23} < \pi/4$ . The dashed curve would be to the left of the solid curve in the left panel if  $\theta_{23} > \pi/4$ .

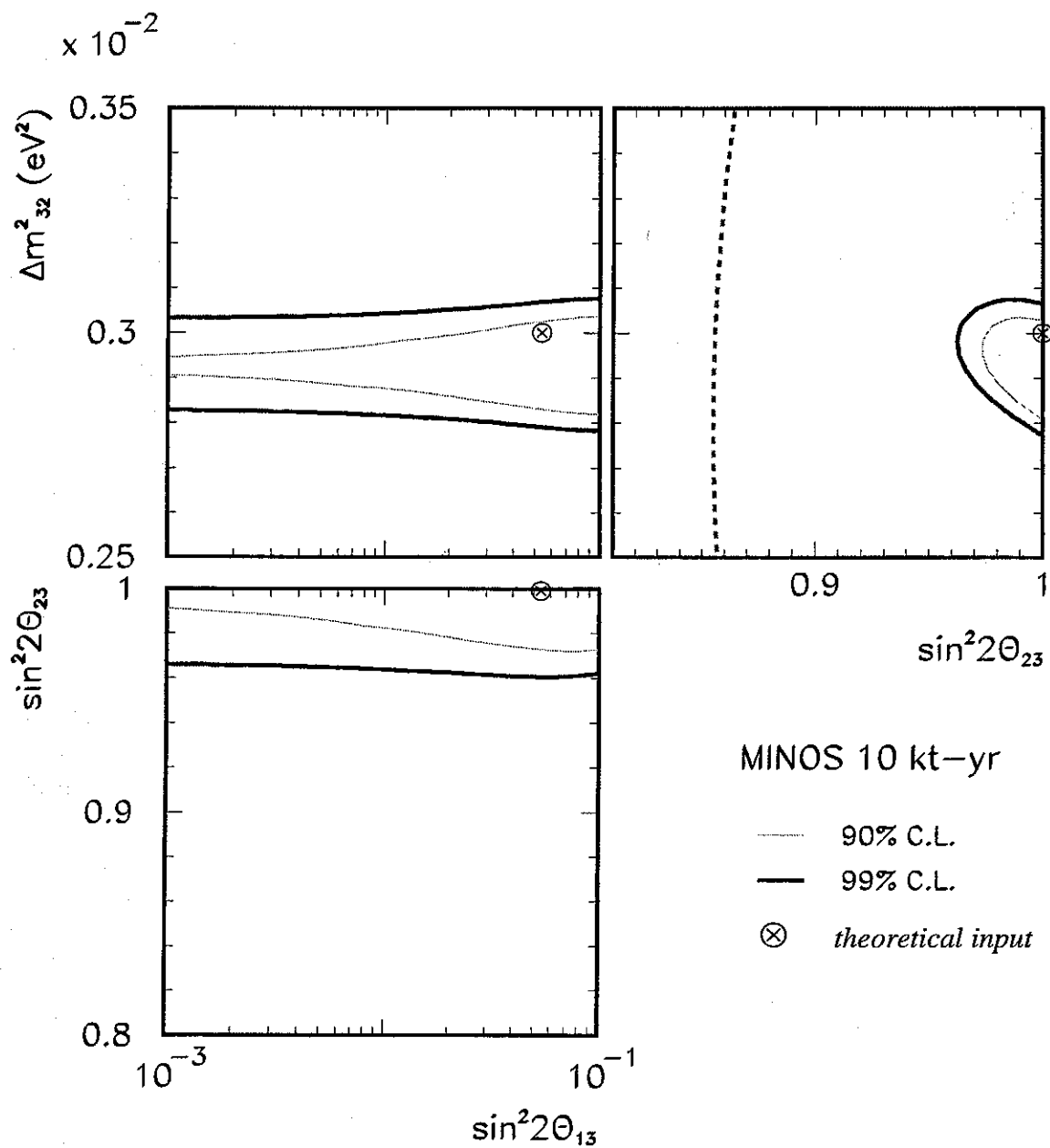


FIG. 2. Expected allowed regions for MINOS at the 90 and 99% C.L. using  $\Delta m_{32}^2 = 3 \times 10^{-3} \text{ eV}^2$ ,  $\Delta m_{21}^2 = 5 \times 10^{-5} \text{ eV}^2$ ,  $\sin^2 2\theta_{23} = 1$ ,  $\sin^2 2\theta_{12} = 0.8$  and  $\sin^2 2\theta_{13} = 0.05$  as the theoretical input for which data was simulated. The dashed line is the Super-Kamiokande allowed region at the 99% C.L.. Here and in other figures, the best fit point is very close to the theoretical input and is consequently not shown.

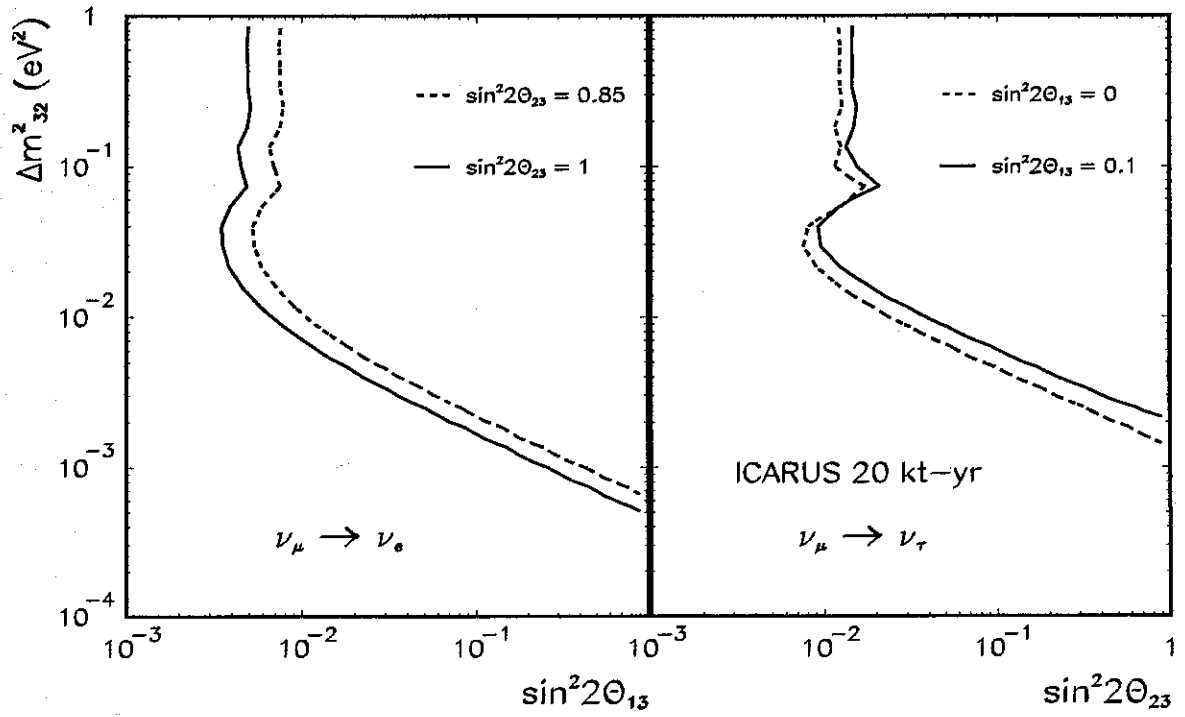


FIG. 3. The same as Fig. 1 but for ICARUS in the  $\nu_\mu \rightarrow \nu_e$  ( $\nu_\tau$ ) oscillation modes.

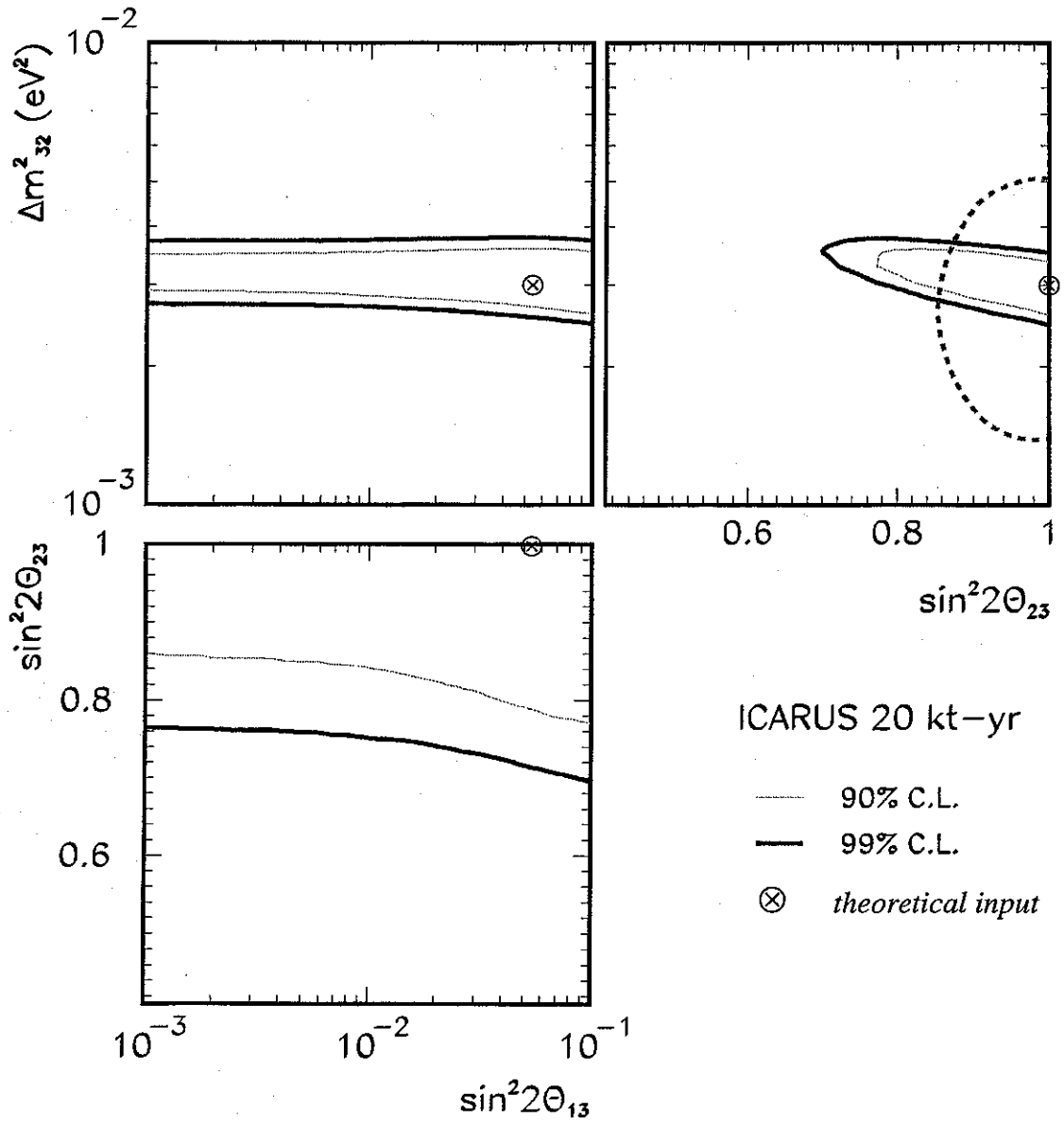


FIG. 4. The same as Fig. 2 but for ICARUS.



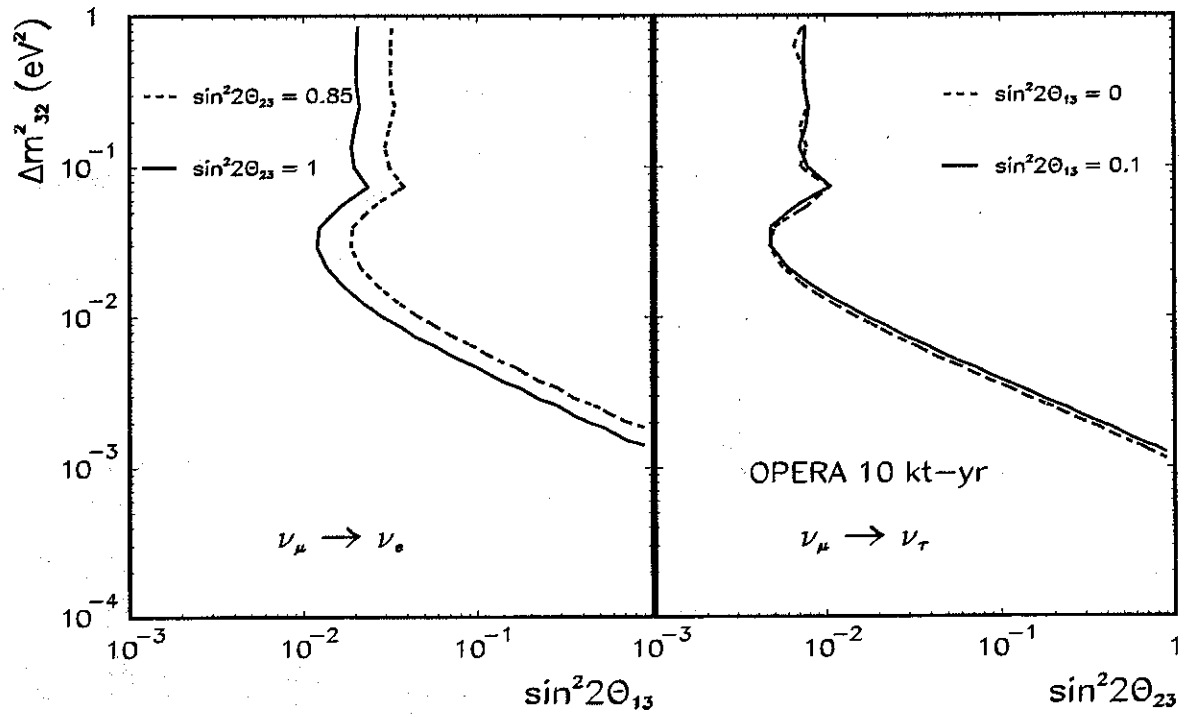


FIG. 5. The same as Fig. 3 but for OPERA.

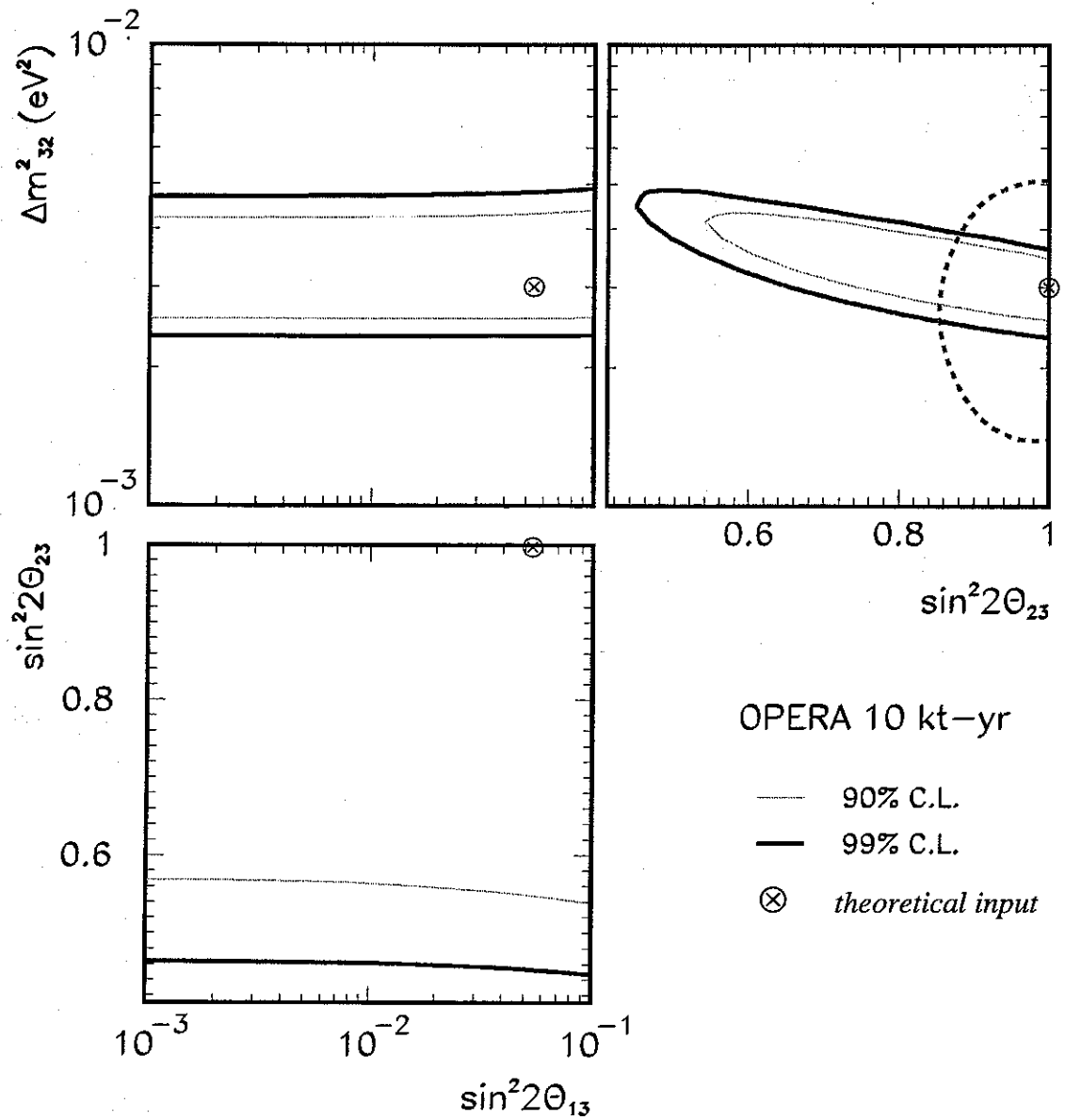


FIG. 6. The same as Fig. 2 but for OPERA.

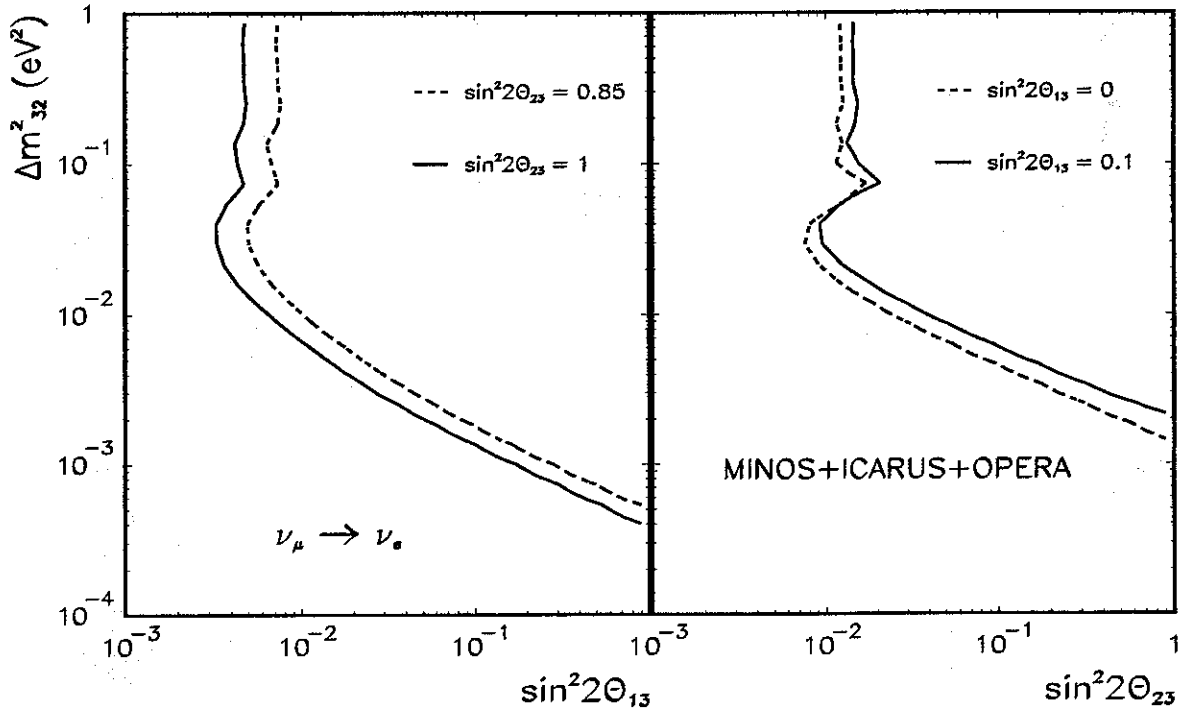


FIG. 7. The global sensitivity of the  $\nu_\mu \rightarrow \nu_e$  mode at 90% C.L. is shown on the left. The sensitivity to  $\sin^2 2\theta_{23}$  and  $\Delta m_{32}^2$  by combining the MINOS sensitivity in the disappearance channel and the ICARUS and OPERA sensitivities in the  $\nu_\mu \rightarrow \nu_\tau$  channels at the 90% C.L. is on the right.

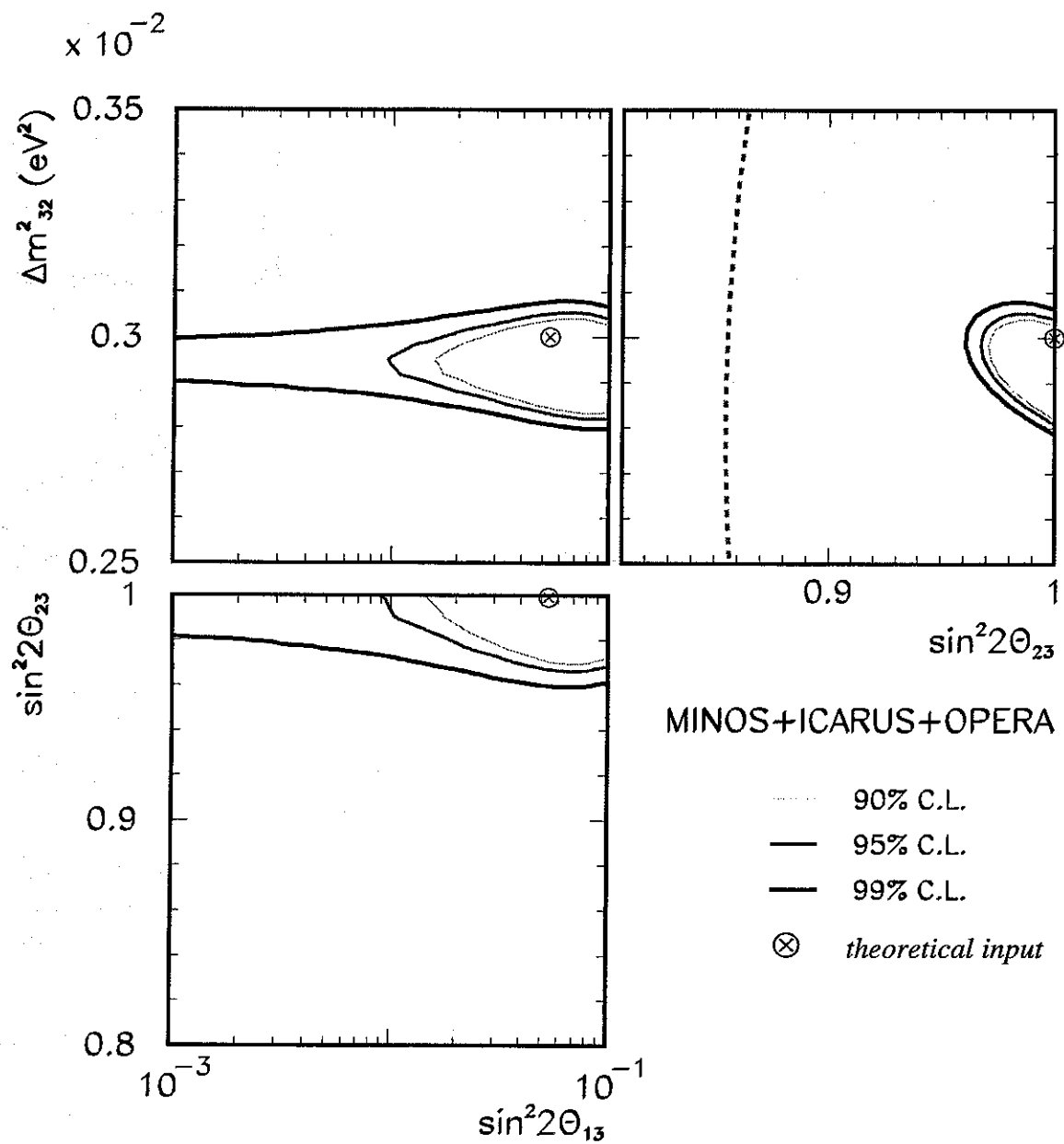


FIG. 8. The same as Fig. 2 but the cumulative simulated data of the three experiments is used and we have also included the 95% C.L. contour.

